Chair and Twist-Boat Membranes in Hydrogenated Graphene

Duminda K. Samarakoon and Xiao-Qian Wang*

Department of Physics and Center for Functional Nanoscale Materials, Clark Atlanta University, Atlanta, Georgia 30314

ABSTRACT Graphane is a two-dimensional system consisting of a single planar layer of fully saturated carbon atoms, which has recently been realized experimentally through hydrogenation of graphene membranes. We have studied the stability of chair, boat, and twist-boat graphane structures using first-principles density functional calculations. Our results indicate that locally stable twist-boat membranes significantly contribute to the experimentally observed lattice contraction. The band gaps of graphane nanoribbons decrease monotonically with the increase of the ribbon width and are insensitive to the edge structure. The implications of these results for future hydrogenated graphene applications are discussed.

KEYWORDS: hydrogenation · graphene · graphane · density functional calculation · nanoribbons

Graphene, a single layer of an all-carbon hexagonal network, is an emerging material for applications in electronics and photonics.[1−4,10−12] As a truly two-dimensional system and a zero-gap semiconductor, where the carriers behave as massless fermions, graphene possesses a number of outstanding electronic properties such as tunable carrier type and density,[2] exceptionally high carrier mobility,[3] quantization of the conductivity,[4] and fractional quantum Hall effect (QHE) even at room temperature.[5] These phenomena, particulary the QHE,[5] have elucidated many important aspects of quantum many-body systems.[5] The corresponding electronic states in graphene promote theoretical advances[6−9] in studying strongly correlated Dirac fermions. Functionalizing graphene by reversible hydrogenation can change the electronic properties from metallic to semiconducting owing to the induced changes of functionalized carbon from sp^2 to sp^3 hybridization.[10−12] The resultant hydrocarbon compound, graphane, can be modified into new materials, fine-tuning its electronic properties, and has opened up increasingly fertile possibilities in hydrogen storage and two-dimensional electronics.[1−4,10−12]

To develop increasingly small and fast transistors, it is desirable to have an energy gap.[2,3] In contrast to complicated graphene-based structures such as quantum point contacts and quantum dots, chemical derivatives of graphene provide a unique tool for controlling electronic properties.[12] In order to utilize their remarkable electronic characteristics, it would be highly desirable to understand the associated electronic structures. On the basis of first-principles density functional calculations, Sofo, Chaudhari, and Barber predicted the stability and semiconducting behavior of graphane,[13] an extended two-dimensional fully saturated hydrocarbon derived from a single graphene sheet.[13,14] Recent experiments by Elias and co-workers[15] demonstrated the graphane formation by exposing pristine graphene to atomic hydrogen. There exist drastic changes in the crystal structure of graphane such that the lattice spacing shrinks by as much as 5%, whereas the hexagonal symmetry remains intact.

The experimentally observed lattice spacing[15] has a significantly broader variation than theoretically studied conformations of graphane.[13,14] Theoretical work has considered two conformations: a chair-like conformer in which hydrogen atoms are alternating on both sides of the plane, and a boat-like conformer in which hydrogen atoms are alternating in pairs.[13,14] In the ground state chair conformation of graphane, hydrogen attaches to graphene sublattices from two opposite sides and carbon atoms in the sublattices move out of the plane that yields the shrinkage of the in-plane periodicity. However, the change in hybridization from sp^2 to sp^3 leads to longer C−C bonds, which surpasses the lattice

*Address correspondence to xwang@cau.edu.

Received for review September 28, 2009 and accepted November 18, 2009.

Published online November 30, 2009.
10.1021/nn901317d

shrinkage by chair membrane buckling. The experimental observation of more compressed areas implies the existence of alternative membranes in the crystal structures of graphane, which results in stronger membrane buckling and shorter in-plane lattice spacing.[15]

Here we present a comprehensive investigation of structural and electronic properties of the graphane and graphane nanoribbons. We employ a combination of classical molecular dynamics[16] and first-principles density functional approach.[17] Classical molecular dynamics was used to prescreen molecular geometries, and first-principles calculations were employed to determine the electronic structure. Our results indicate that the locally stable twist-boat membranes lead to pronounced lattice shrinkage and thus contribute to the broader distribution of lattice spacing observed experimentally.[15] The incorporation of twist-boat membranes into the crystal structure of graphane is shown to preserve the semiconducting feature of graphane. Furthermore, a systematic study of the graphane nanoribbons shows that the band gaps of graphane nanoribbons decrease monotonically with the increase of the ribbon width and are insensitive to the edge structure.

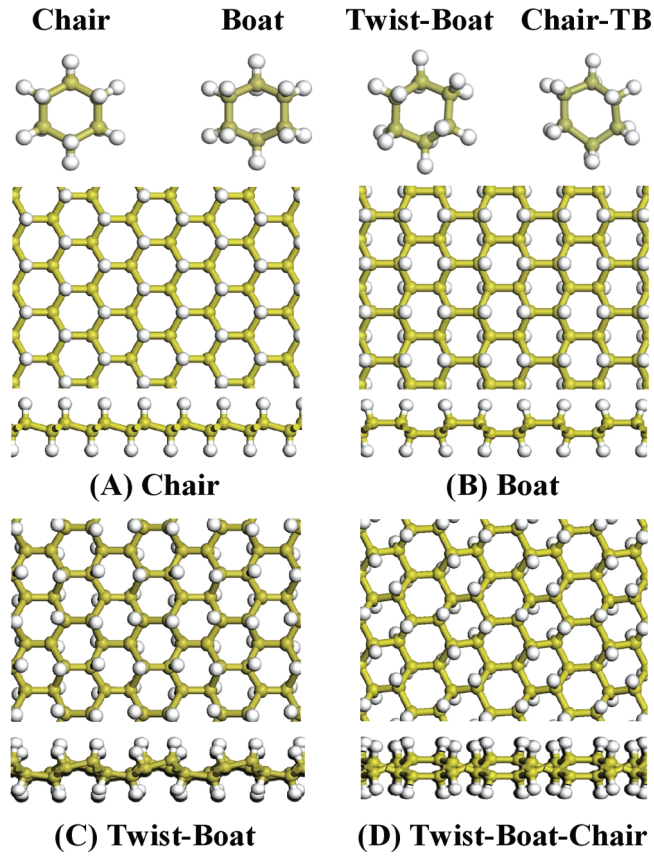

Figure 1. Top panel: top view of chair, boat, twist-boat, and chair-twist-boat conformations of cyclohexane. Carbon atoms are shown as gold, and hydrogen atoms are white. Middle and bottom panels: top and side views of graphane conformations for (A) chair, (B) boat, (C) twist-boat, and (D) twist-boat-chair.

We have performed first-principles calculations for various graphane structures. The structure and electronic properties of all conformations were investigated using first-principles density functional calculations. Perdew−Burke−Ernzerhof parametrization[18] of the generalized gradient approximation was used in all of the calculations. A kinetic energy cutoff of 280 eV in the plane-wave basis and appropriate Monchorst−Pack *k*-points ($6 \times 6 \times 1$ for graphane and $10 \times 1 \times 1$ for graphane nanoribbons) were sufficient to converge the grid integration of the charge density. Although the first-principles approach systematically underestimates the band gaps,[19] we are interested primarily in the general feature of the conformations or membranes. The initial search for stable structures was carried out through classical molecular dynamics by means of Tersoff potential.[16] The obtained local energy-minimum structures were further optimized through first-principles calculations with forces less than 0.01 eV/Å.

In order to effectively search for stable crystal structures of graphane, it is instructive to make reference to distinctive configurations of cyclohexane (see top panel of Figure 1) referred to as chair, boat, twist-boat, and chair-twist-boat. Due to the inherent tendency of the sp^3 hybridization on tetravalent carbons, cyclohexane does not form a planar hexagonal arrangement. The chair isomer is the ground state configuration, while twist-boat is the second lowest-energy isomer. The chair conformation changes in the ring-flipping process, leading to the axial hydrogens becoming equatorial. Between the two stable chair states (with D_{3d} symmetry), the twist-boat (with D_2 symmetry), boat (with C_{2v} symmetry), and chair-twist-boat isomers can be constructed. The boat and chair-twist-boat forms are metastable states of the twist and chair forms, respectively. The twist-boat form may be isolable because—like the chair form—it stands for an energy minimum. The boat conformation is free from angle strain but has a higher energy than the chair form due to steric strain in connection to the flagpole interaction. The torsional strain in the boat conformation has a maximum value since two of the carbon bonds are fully eclipsed. This is to be contrasted to the chair conformer in which all bonds are staggered and complete absence of torsional strain, while the twist-boat has four partially eclipsed bonds.

The counterparts of chair, boat, and twist-boat conformers of cyclohexane in two-dimensional structures of graphane can be constructed accordingly. We illustrate in Figure 1 the structures of chair, boat, and twist-boat conformations of graphane, along with a twist-boat-chair structure. The chair and boat structures coincide with configurations previously obtained using

TABLE 1. Calculated Binding Energy Per Carbon Atom E_B, Band Gap E_g, Bond Length a, Associated Planar Projection a_0, the In-Plane Lattice Spacing d for Chair, Boat, Twist-Boat(TB)-Chair Conformations of Graphane, Respectively

structure	E_B (eV)	E_g (eV)	a (Å)	a_0 (Å)	d (Å)
graphene	−8.57	0	1.42	1.42	2.47
chair	−12.23	3.5	1.54	1.47	2.55
boat	−12.06	3.5	1.54, 1.58	1.40, 1.58	2.51, 2.54
TB-chair	−11.97	3.8	1.53−1.57	0.89−1.51	2.45−2.60

density functional calculations.[13,14] The unit cell of the chair and boat conformation has $P3\bar{m}1$ and $Pmmn$ symmetries, respectively. Consistent with the energy order of cyclohexane, the chair configuration is lower in energy and has less membrane buckling than those of the boat conformer.

The twist-boat configuration of graphane has more in-plane shrinkage than either chair or boat conformation. However, the twist-boat structure becomes unstable against the boat conformation in geometry optimization using first-principles calculations. Closer scrutiny of the geometry optimization process from a twist-boat structure of graphane to the boat configuration reveals that the additional energy cost is attributed to the fact that all carbon atoms in the unit cell participate in the bond-twisting process. By contrast, in cyclohexane, only four out of six carbon atoms mimicking a pair of twist bonds are involved in the optimization between boat and twist-boat forms.

It becomes clear that the experimentally observed graphane is unlikely to be in the single-crystal form of chair, boat, or twist-boat because each of those structures has only one or two distinctive in-plane lattice spacing, in contrast to a wide range of distributions observed experimentally.[15] Moreover, the twist-boat configuration is no longer stable against the boat structure. However, the instability of the twist-boat crystal structure does not preclude the existence of locally stable twist-boat membranes. To pursue this scenario, we show in Figure 1 a twist-boat-chair configuration, which consists of adjacent twist-boat and chair membranes. Our first-principles calculation shows that the twist-boat-chair configuration is a stable structure of graphane, although the energy is slightly higher than the boat and chair conformations. Summarized in Table 1 are the structural and electronic properties of the conformation as compared to those for graphene as well as chair and boat conformations of graphane. It is worth noting that, in the twist-boat-chair configuration, locally stable twist-boat membranes are favored over boat ones since two carbon atoms in the membrane serve as linkage atoms for the neighbor chair membranes. The unit cell of twist-boat-chair structure has a P_2/c symmetry with monoclinic angle $\gamma = 138.5°$.

An important ramification of our investigation of various graphane crystal structures is that the low energy conformations have no more than one parallel

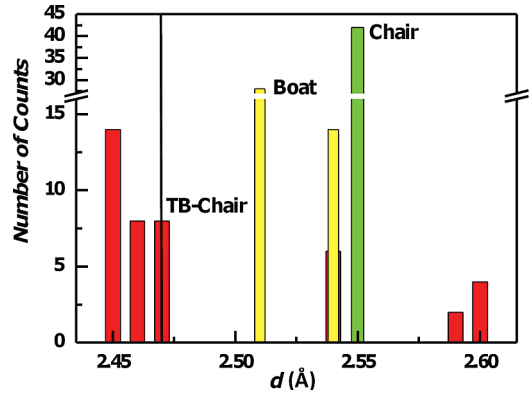

Figure 2. Number of counts (collected from a sample with 42 lattice spacings) of in-plane lattice spacing for chair (green), boat (yellow), and twist-boat-chair (red) conformations of graphane. The vertical solid line corresponds to theoretical in-plane lattice spacing of graphene.

aligned nearest-neighbor hydrogen, as the hydrogen in the chair and boat has zero and one parallel aligned neighbor, respectively. On the other hand, the chair membranes in the twist-boat-chair structure may have two neighboring hydrogens. This trend is also observable for various other stable structures of graphane. We depict in Figure 2 the distribution of lattice spacing for various crystal structures of graphane. For the chair conformation, there exists only one distinctive lattice spacing. For the boat conformer, there are two distinctive in-plane lattice spacings. The twist-boat-chair conformation has a broad range of in-plane lattice spacings from 2.45 to 2.60 Å. The lowest lattice spacing of 2.45 Å is about 1% of lattice contraction as compared with the value obtained for graphene (2.47 Å), which is about 5% contraction of the value for chair (2.55 Å). This contraction can be correlated to short in-plane bond lengths which can be as small as 0.89 Å (see Table 1).

The transformation among various graphane structures amounts to flipping hydrogens from one side of the plane to another, along with the associated strain relaxation for the carbon atoms attached. The transition states are characterized with distortions of the hexagonal network with elongated carbon bonds in order to accommodate hydrogens that are in the network plane during the flipping process. This implies that once the hydrogens are absorbed onto graphene with full saturation it becomes difficult for the system to adopt the ground state chair conformation. As a result, the sequence of alternating hydrogens on both sides of the plane is broken, introducing other types of membranes into the crystal structure of graphane. Consequently, this leads to out-of-plane distortions that induce in-plane shrinkage and results in a decrease of the in-plane lattice spacing in relation to that of the chair conformation.

We believe that the experimentally observed broad distribution of lattice spacings can be attributed, to a large extent, to the existence of membranes other than the chair form. In this regard, locally stable twist-boat

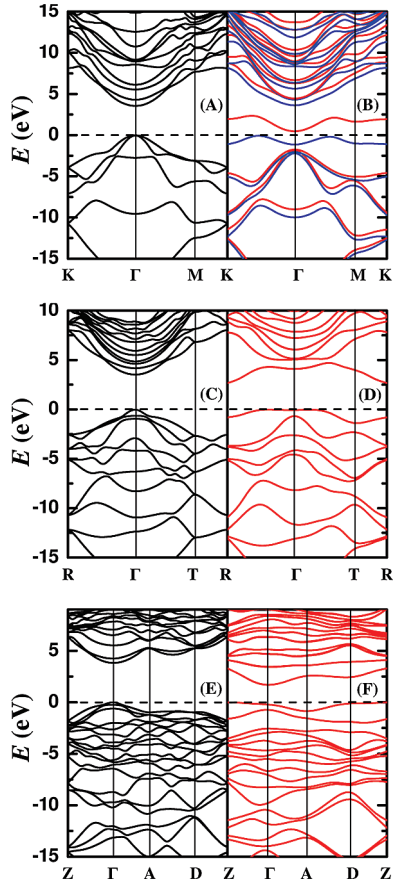

Figure 3. Calculated band structure for (A) chair, (C) boat, and (E) twist-boat-chair conformations of graphane, and their counterparts (B), (D), and (F) for one-side half-hydrogenated graphene (graphone), respectively. The red and blue curves represent spin-up and spin-down components, respectively. For chair conformation, K = (π/3a, 2π/3a), M = (0, π/2a), where a = 2.55 Å. For boat conformation, R = (π/2b_1, π/2b_2), T = (π/2b_1, 0), where b_1 = 2.55 Å and b_2 = 4.33 Å. For twist-boat-chair conformation, Z = (0, π/2c_2), A = (π/2c_1, 0), D = (π/2c_1, π/2c_2), where c_1 = 6.63 Å and c_2 = 4.92 Å. The valence band maximum is set to 0 eV.

membrane, as exemplified in twist-boat-chair, is the prototype of low energy configurations with parallel-aligned nearest-neighbor hydrogens. Furthermore, as exemplified in the twist-boat-chair structure, the twist-boat conformer serves as an effective link to neighboring chair conformers.

The band gap of the twist-boat-chair structure, together with that of the chair and boat conformations, can be extracted from the corresponding band structures illustrated in Figure 3. The band structure for twist-boat-chair resembles an interpolation of those of chair and boat ones, and the corresponding band gap of 3.8 eV is very close to those obtained for chair and boat structures.[13,14] In all of the cases, the graphane structures have direct gaps at the band center (Γ point).

Recently, structures with one-sided hydrogenation that are reminiscent of hydrogenation on epitaxial graphene[20] or graphene on a substrate have attracted a great deal of attention.[15] Of particular interest is the recent theoretical prediction that semihydrogenated

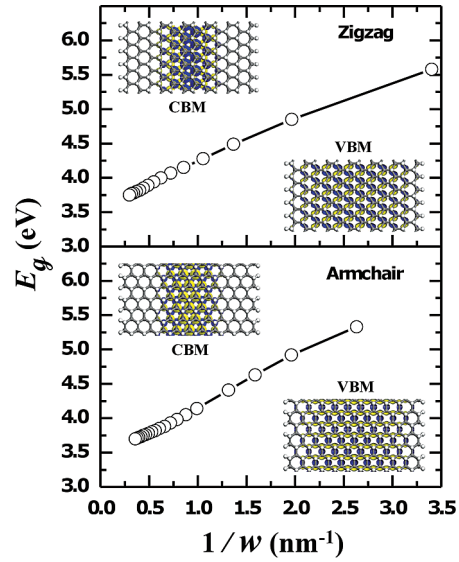

Figure 4. Calculated band gaps of nanoribbons of graphane with zigzag (top panel) and armchair (bottom panel) edges. Insets: extracted charge density distribution at the band center (Γ point) of the corresponding CBM and VBM states.

graphene (graphone) becomes a ferromagnetic semiconductor with a small indirect gap.[21] The half-hydrogenation in the chair conformation breaks the delocalized π bonding network of graphene, leaving the electrons in the unhydrogenated carbon atoms localized and unpaired. While the idea of a ferromagnetic semiconducting graphone is extremely provocative, a careful examination of various graphone configurations is necessary. Our calculation of the chair, boat, and twist-boat-chair conformations of graphone reveals that the ferromagnetic state with an indirect gap of 0.51 eV (see Figure 3B) is very fragile. An implication is that spin-polarized valence band maximum states show long-range correlations and thus depend on the size of the unit cell studied. On the other hand, the ground state of boat and twist-boat-chair conformations is nonmagnetic (Figure 3D,F). Moreover, in contrast to graphane in that the chair configuration is the lowest energy configuration, the energy for boat graphone of −9.88 eV is lower than that of −9.42 eV for chair graphone.

The reason for a band gap opening up in hydrogenated graphene can be attributed to the changes from sp^2-bonded C atoms to sp^3-bonded ones.[13] We have found that all the fully saturated graphane structures have a wide gap, including graphane nanoribbons. Shown in Figure 4 is the dependence of band gaps on the width of the graphane nanoribbon with armchair and zigzag edges. The naming of the armchair and zigzag nanoribbons follows the edge structure nomenclature, such that an armchair (zigzag) tube unfolds into a zigzag (armchair) ribbon.[22,23] The ribbons involved in the present study were constructed based on chair conformations and were neutral bond saturated with hydrogen passivation at edges.

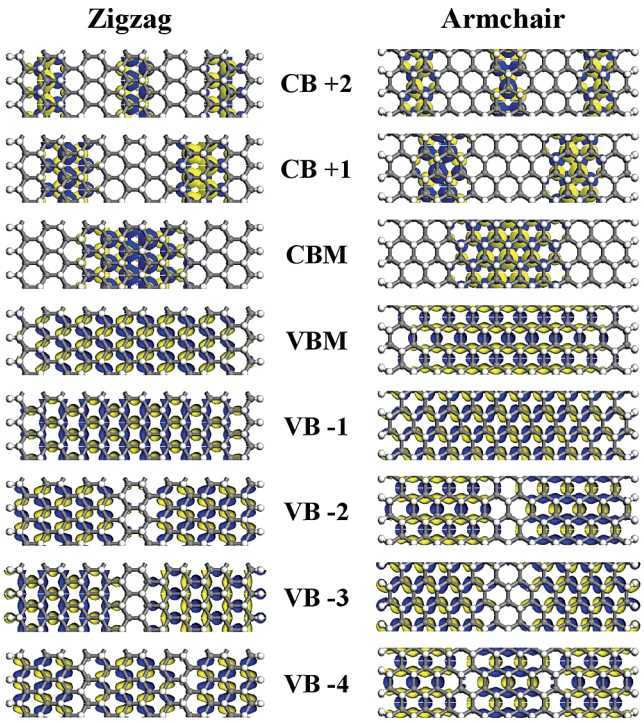

Figure 5. Charge density distributions of near gap conduction and valence states for armchair (left panels) and zigzag (right panels) edged graphane nanoribbons, respectively. The sign of the wave function is indicated by light blue and yellow regions, respectively. The isovalue is 0.025 au.

As is readily observable in Figure 4, the gaps of the ribbon decrease with increasing width w in an approximate $1/w$ fashion. The extracted charge density distribution of the conduction band minimum (CBM) and valence band maximum (VBM), as seen from insets of Figure 4, indicates predominantly confined electrons and holes in the proximity of the ribbon center. The calculated gaps are insensitive to the details of the ribbon edge geometry and termination, in sharp contrast to sp^2-bonded graphene nanoribbons (GNRs). The band gap of ultrathin GNR with armchair edges generally opens up due to the quantum confinement and the edge bond relaxation. The oscillatory band gap for GNR with armchair edges can be explained by the Fermi wavelength in the direction normal to the ribbon direction.[22,23] Similar to zigzag SWNTs, the band gaps of AGNRs are divided into three groups, with the $3p + 2$, $3p + 1$, and $3p$ group (p is a positive integer) having a small, medium, and large gap, respectively.[22,23] It is worth noting that the oscillatory behavior of sp^2-bonded GNRs completely disappears for sp^3-bonded graphane nanoribbons.[24] Furthermore, our calculations based on spin-polarized calculations confirmed that the ground state of graphane nanoribbons with zigzag edges is not magnetic, in contrast to the staggered antiferromagnetic state for zigzag GNRs.[22]

The extracted density distribution of holes and electrons for graphane nanoribbons with zigzag and armchair edges is illustrated in Figure 5. For conduction bands, the near gap states exhibit s, p, d, ... characters, in conformity with predictions from one-dimensional particle-in-a-box model.[25] The s, p, d, ... features are also observable for valence states but for a pair of nearly degenerate (at the band center) valence bands. The close resemblance of the charge distributions for zigzag and armchair edged graphane nanoribbons indicates that edge effect becomes dormant for sp^3-bonded ribbons. These results suggest that by tailoring the effective ribbon width it is feasible to design semiconductor graphane nanoribbons with a tunable band gap, which is advantageous over GNRs in that one can avoid the daunting task of identifying the edge structures. Accordingly, the control of proper nanostructures may offer avenues for the design of highly effective nanodevices.

The approach described in the present work can be employed to investigate hydrogenated graphene systems, such as patterned graphene nanoroads[26] that are composed of GNRs with fully saturated hydrogenation at the edges and well-defined sharp interfaces between sp^2- and sp^3-bonded membranes. Of particular interest is the interplay between sp^2 and sp^3 hybridizations that can be systematically investigated *via* band alignment analysis. The band alignment for patterned graphene nanoroads is based on the lineup of charge neutrality levels[27] for sp^2- and sp^3-bonded components. Since sp^3 hybridization leads to wide gap semiconducting behavior, the electronic properties of patterned nanoroads are primarily determined by the sp^2 components. For instance, for graphene nanoroads with armchair edges, the band gaps are in accordance with results of GNRs with the effective sp^2 width and show oscillatory behavior.[26]

In summary, we have studied various stable crystal structures of graphane and demonstrated that locally stable twist-boat membranes significantly contribute to the experimentally observed lattice contraction. The first-principles results shed considerable light on the electronic characteristics associated with the sp^3 hybridization. Moreover, the first-principles approach can be employed to structural and electronic properties of hydrogenated graphene derivatives. The understanding of structural and electronic stability thus provides a useful means for future development of graphane-based nanodevices.

Acknowledgment. This work was supported in part by the National Science Foundation (Grant No. DMR-0934142) and Army Research Office (Grant No. W911NF-06-1-0442).

REFERENCES AND NOTES

1. Geim, A. K.; Novoselov, K. S. The Rise of Graphene. *Nat. Mater.* **2007**, *6*, 183.

2. Berger, C.; Song, Z.; Li, X.; Wu, X.; Brown, N.; Naud, C.; Mayou, D.; Li, T.; Hass, J.; Marchenkov, A. N.; Conrad, E. H.; First, P. N.; de Heer, W. A. Electronic Confinement and Coherence in Patterned Epitaxial Graphene. *Science* **2006**, *312*, 1191.
3. Zhang, Y.; Jiang, Z.; Small, J. P.; Purewal, M. S.; Tan, Y.-W.; Fazlollahi, M.; Chudow, J. D.; Jaszczak, J. A.; Stormer, H. L.; Kim, P. Landau-Level Splitting in Graphene in High Magnetic Fields. *Phys. Rev. Lett.* **2006**, *96*, 136806.
4. Novoselov, K. S.; Geim, A. K.; Morozov, S. V.; Jiang, D.; Katsnelson, M. I.; Grigorieva, I. V.; Dubonos, S. V.; Firsov, A. A. Two-Dimensional Gas of Massless Dirac Fermions in Graphene. *Nature* **2005**, *438*, 197.
5. Zhang, Y.; Tan, Y. W.; Stormer, H. L.; Kim, P. Experimental Observation of the Quantum Hall Effect and Berry's Phase in Graphene. *Nature* **2005**, *438*, 201.
6. Laughlin, R. B. Anomalous Quantum Hall Effect: An Incompressible Quantum Fluid with Fractionally Charged Excitations. *Phys. Rev. Lett.* **1983**, *50*, 1395.
7. Jain, J. K. Composite-Fermion Approach for the Fractional Quantum Hall Effect. *Phys. Rev. Lett.* **1989**, *63*, 199.
8. Halperin, B.; Lee, P. A.; Read, N. Theory of the Half-Filled Landau Level. *Phys. Rev. B* **1993**, *47*, 7312.
9. Ciftja, O.; Fantoni, S. A New Hypernetted-Chain Treatment for Laughlin Quantum Hall States. *Europhys. Lett.* **1996**, *36*, 663.
10. Geim, A. K.; Morozov, S. V.; Hill, E. W.; Blake, P.; Katsnelson, M. I.; Novoselov, K. S. Detection of Individual Gas Molecules Adsorbed on Graphene. *Nat. Mater.* **2007**, *6*, 652.
11. Wang, X.; Zhi, L.; Mullen, K. Transparent, Conductive Graphene Electrodes for Dye-Sensitized Solar Cells. *Nano Lett.* **2008**, *8*, 323.
12. Gilje, S.; Han, S.; Wang, M.; Wang, K. L.; Kaner, R. B. A Chemical Route to Graphene for Device Applications. *Nano Lett.* **2007**, *7*, 3394.
13. Sofo, J. O.; Chaudhari, A. S.; Barber, G. D. Graphane: A Two-Dimensional Hydrocarbon. *Phys. Rev. B* **2007**, *75*, 153401.
14. Boukhvalov, D. W.; Katsnelson, M. I.; Lichtenstein, A. I. Hydrogen on Graphene: Electronic Structure, Total Energy, Structural Distortions and Magnetism from First-Principles Calculations. *Phys. Rev. B* **2008**, *77*, 035427.
15. Elias, D. C.; Nair, R. R.; Mohiuddin, T. M. G.; Morozov, S. V.; Blake, P.; Halsall, M. P.; Ferrari, A. C.; Boukhvalov, D. W.; Katsnelson, M. I.; Geim, A. K.; Novoselov, K. S. Control of Graphene's Properties by Reversible Hydrogenation: Evidence for Graphane. *Science* **2009**, *323*, 610.
16. Tersoff, J. New Empirical Approach for the Structure and Energy of Covalent Systems. *Phys. Rev. B* **1988**, *37*, 6991.
17. Kresse, G.; Furthmuller, J. Efficient Iterative Schemes for *Ab Initio* Total-Energy Calculations Using a Plane-Wave Basis Set. *Phys. Rev. B* **1996**, *54*, 11169.
18. Perdew, J. P.; Burke, K.; Ernzerhof, M. Generalized Gradient Approximation Made Simple. *Phys. Rev. Lett.* **1996**, *77*, 3865.
19. Yang, L.; Cohen, L. M.; Louie, G. S. Magnetic Edge-State Excitons in Zigzag Graphene Nanoribbons. *Phys. Rev. Lett.* **2008**, *101*, 186401.
20. Guisinger, N. P.; Rutter, G. M.; Crain, J. N.; First, P. N.; Stroscio, J. A. Exposure of Epitaxial Graphene on SiC(0001) to Atomic Hydrogen. *Nano Lett.* **2009**, *9*, 1462.
21. Zhou, J.; Wang, Q.; Sun, Q.; Chen, X. S.; Kawazoe, Y.; Jena, P. Ferromagnetism in Semihydrogenated Graphene Sheet. *Nano Lett.* **2009**, *9*, 3867.
22. Son, Y.-W.; Cohen, M. L.; Louie, S. G. Energy Gaps in Graphene Nanoribbons. *Phys. Rev. Lett.* **2006**, *97*, 216803.
23. Barone, V.; Hod, O.; Scuseria, G. E. Electronic Structure and Stability of Semiconducting Graphene Nanoribbons. *Nano. Lett.* **2006**, *6*, 2748.
24. Li, Y.; Zhou, Z.; Shen, P.; Chen, Z. Structural and Electronic Properties of Graphane Nanoribbons. *J. Phys. Chem. C* **2009**, *113*, 15043.
25. Nduwimana, A.; Musin, R. N.; Smith, A. H.; Wang, X.-Q. Spatial Carrier Confinement in Core−Shell and Multishell Nanowire Heterostructures. *Nano Lett.* **2008**, *8*, 3341.
26. Singh, A. K.; Yakobson, B. I. Electronics and Magnetism of Patterned Graphene Nanoroads. *Nano Lett.* **2009**, *9*, 1540.
27. Nduwimana, A.; Wang, X.-Q. Charge Carrier Separation in Modulation Doped Coaxial Semiconductor Nanowires. *Nano Lett.* **2009**, *9*, 283.